The modified nodal equations are obtained as follows:

$$\begin{bmatrix} 0 & 0 & 0 & 0 & 0 & 0 & 0 & -1 & 1 \\ 0 & 1/R_L & -1/R_L & 0 & 0 & 0 & 0 & 0 & -1 \\ 0 & -1/R_L & 1/R_L & 0 & 0 & 1 & 1 & 0 & 0 \\ 0 & 0 & 0 & sC+1/R & -sC & -1 & 0 & 0 & 0 \\ 0 & 0 & 0 & -sC & sC+1/R_c & 0 & 0 & 0 & 0 \\ 0 & 0 & 1-\alpha & -1+\alpha & 0 & \alpha & 0 & 0 & 0 \\ 0 & 0 & \alpha-\beta & 0 & 0 & 0 & 1-\alpha+\beta & 0 & 0 \\ -1 & 0 & 0 & 0 & 0 & 0 & 0 & 0 & 0 \\ 1 & -1 & 0 & 0 & 0 & 0 & 0 & 0 & -sL \end{bmatrix} \begin{bmatrix} V_{10} \\ V_{20} \\ V_{30} \\ V_{40} \\ V_{50} \\ I_1 \\ I_2 \\ I_7 \\ I_8 \end{bmatrix} = \begin{bmatrix} 0 \\ 0 \\ 0 \\ Cy_c(t_0) \\ 0 \\ 0 \\ 0 \\ -V_g/s \\ -Li_L(t_0) \end{bmatrix}$$

Solving the equations, the line to output transfer function $V_{50}(s)/(V_g/s)$, and then the transient response $v_{50}(t)$, may be analytically found. The expression obtained contains the time-variable parameters α and β. By particularising α and β for each switching interval, partial analytic, continuous solutions are obtained. These expressions are used in accordance with the algorithm presented in Reference 3 for computing the convertor global response. The result is both exact (as in sampled-data methods) and time-continuous (as in averaging methods), as in each interval the solution is known analytically. This is the first advantage of the 'alternor' approach.

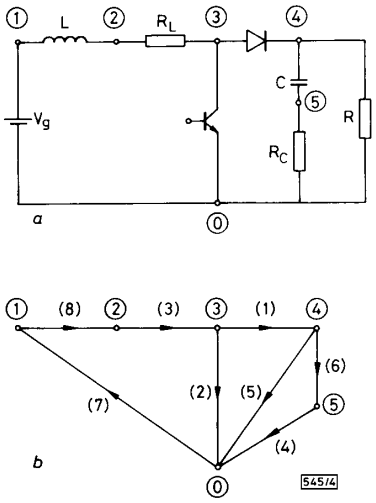

Fig. 4 *DC/DC buck convertor and its graph*

Despite the fact that the solution is not obtained in closed form, the above approach has a second advantage: unlike all the available methods,[3] in which a set of equations is found for each switching configuration (and three or more intervals per cycle are possible in the operation of power electronics circuits) necessitating the computation of a corresponding number of partial solutions, in the 'alternor' approach, only one modified nodal equations set is obtained, describing the global behaviour of the convertor; one solution of this system is found and is then particularised for suitable values of α and β. Such an approach permits the automatisation and the computer implementation of the method.

A. IOINOVICI* *7th December 1987*

Department of Electrical Engineering
Centre for Technological Education
Holon, Holon 58102, Israel

* Also with Weizmann Institute of Science, Rehovot, Israel

References

1 IOINOVICI, A.: 'Exact transient solution of the boost converter computed using the alternor equations', *Int. J. Electronics* (in press)
2 MIDDLEBROOK, R. D., and CUK, S.: 'Advances in switched-mode power conversion' (Teslaco, Pasadena, 1983)
3 IOINOVICI, A., and SHENKMAN, A.: 'Design-oriented analysis of common switching DC to DC converters', *Int. J. Electronics*, 1987, **62**, pp. 923–933

FAST DIRECT e-BEAM LITHOGRAPHIC FABRICATION OF FIRST-ORDER GRATINGS FOR 1·3 μm DFB LASERS

Indexing terms: Lasers and laser applications, Semiconductor lasers, Electron-beam lithography

Phase-shifted first-order gratings for 1·3 μm distributed-feedback (DFB) lasers have been fabricated in InP by fast direct e-beam lithography. The two-layer resist system consisted of a highly sensitive (~3 μC/cm²) positive organosilicon e-beam resist, poly(3-butenyltrimethylsilane sulfone) (PBTMSS), and a bottom layer of diamond-like carbon (DLC). The high quality of these gratings was reflected in the excellent characteristics of the DFB lasers.

Introduction: Diffraction gratings fabricated in optoelectronic and semiconductor materials are integral components in certain devices, such as the distributed-feedback (DFB) lasers used in the present and future optical communication systems. In a DFB laser, a grating containing a $\lambda/4$ shift permits single-frequency operation of the laser, which is necessary for the coherent lightwave systems of the future.

DFB laser gratings have been generally fabricated by the holographic interference method.[1] However, the resist profile resulting from the holographic exposure is sinusoidal which imposes a narrow processing latitude on the fabrication process. Further, experimental procedures for introducing $\lambda/4$ shifts[2–4] and other features are complicated.

Electron-beam lithography, on the other hand, has resolution significantly better than the 0·07–0·12 μm required to fabricate first-order gratings for DFB lasers. However, lack of a suitable resist has precluded wider exploitation of e-beam lithography in such applications. Poly(methyl methacrylate) (PMMA), the traditional resist of choice for high-resolution pattern definition, has a sensitivity (300–400 μC/cm² for 230 nm-period gratings)[6] that is far too low to permit a practical writing speed. In addition, the lack of stability of PMMA and other more sensitive e-beam resists in various wet- and dry-etching environments poses a difficult processing problem.

The latter problem has been alleviated by the introduction of multilayer resist systems.[7] For example, Kakuchi *et al.*[8] reported the fabrication of 200 nm-period gratings in silicon using chloromethylated poly(diphenylsiloxane) negative e-beam resist ($D_{0.8} = 120\,\mu C/cm^2$) in conjunction with diamond-like carbon (DLC) films as the bottom layer of the two-layer structure.

We have developed a two-layer process for fabricating DFB laser gratings using the sensitive positive organosilicon e-beam resist, poly(3-butenyltrimethylsilane sulfone) (PBTMSS).[9] In an accompanying paper, we report detailed characteristics of single-mode DFB DC-PBH lasers incorporating such gratings.[12]

Process: The basic fabrication steps are outlined in Fig. 1. They include coating a precleaned InP substrate with the two-layer resist system, exposing and developing the top e-beam resist layer, transferring the pattern into the bottom layer by O_2 RIE, etching the substrate, and stripping the resist. Details of the synthesis and lithographic performance of PBTMSS have been reported previously.[9,10]

PBTMSS rapidly degrades in all dry etching environments with the exception of an oxygen plasma; thus the bottom layer serves as the proper etch mask during etching of the substrate. Since the spin-coating of 100 to 200 nm-thick polyimide films was often irreproducible, DLC films deposited by plasma cracking[11] of 1,3-butadiene were used as the bottom layer. The films were deposited at a pressure of 20 mtorr, using a 13·56 MHz parallel-plate RIE reactor (RF power = 25 W, self-bias = −580 V, deposition rate ≈ 100 nm/min).

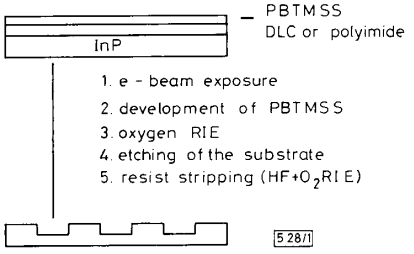

Fig. 1 *Two-layer resist process used to fabricate first-order diffraction gratings for 1·3 μm DFB-DCPBH lasers*

50 nm-thick films of PBTMSS ($M_n = 5 \times 10^5$, $M_w/M_n \approx 2$) were deposited on the substrate by spin-coating, and exposed with a 25 keV electron beam using a JEOL JBX 5D II(U) electron-beam exposure system employing a single-crystal LaB_6 filament. The lines were exposed with a single pass of a 20 nm-diameter beam using exposure times of 1·4 and 2·8 μs/spot for beam currents of 100 and 50 pA, respectively. The lines were written by a series of spot exposures using a 20 nm increment between the exposed spots. The average area dose was ≃3·5 μC/cm^2. The exposed samples were dip-developed in a 9 : 1 mixture of 2-propanol (IPA) and 2-butanol for 45 s at 10°C followed by a 5 s rinse in IPA and drying in a stream of dry nitrogen.

In the next step, the pattern defined in the top layer of PBTMSS was transferred into the bottom DLC layer by O_2 RIE. As we have shown in earlier work,[10] the PBTMSS resist requires 'passivation' before etching under 'standard' O_2 RIE conditions. This process involves increasing the RF power during the initial 10 s of etching to maintain a self-bias voltage between −550 and −600 V. After this short period, the RF power level is reduced, resulting in self-bias of −350 V in our instrument. Under such conditions, the resist surface is rapidly converted into a compact and uniform SiO_2 layer, and the concomitant resist degradation by volatilisation is significantly reduced. Fig. 2 shows an SEM micrograph of a 200 nm-period grating in the resist including the λ/4 shift.

Due to the exceptional mechanical and chemical stability of DLC films, any dry- or wet-etching technique can be used to etch the grating pattern in the InP substrate. The gratings used in the DFB lasers fabricated in our laboratory[12] were etched using 10 wt.-% aqueous iodic acid solution for 15 s, followed by a rinse in deionised water and drying (Fig. 3). The grating lines were oriented along the [010] direction. The etching process was designed to yield a symmetric grating of equal line and spacing to maximise the coupling coefficient, κ.

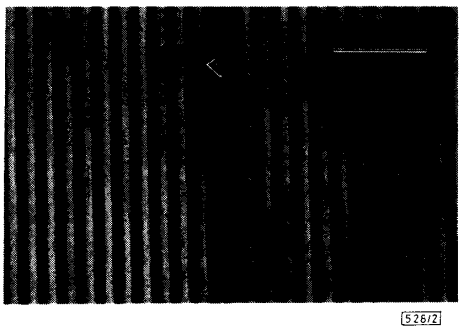

Fig. 2 *Grating incorporating λ/4-shift (arrow) after O_2 RIE pattern transfer into polyimide*

Scale bar = 1 μm

Much deeper grooves without undercut were made using ion-beam-assisted etching with a 150 mA/cm^2 argon-ion beam in an iodine monochloride reactive gas flux (Fig. 4). This dry-etching technique allows anisotropic etching of InP and GaInAsP at etch rates ranging from 10 to 1000 nm/min. The small irregularities seen in the etched grooves most probably result from the crystallographic selectivity of the etchant, since no corresponding features were seen in the DLC pattern. Other authors have reported similar observations.[6]

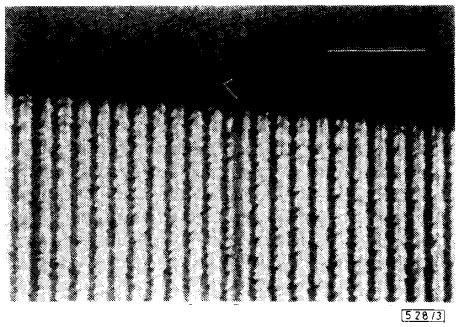

Fig. 3 *SEM micrograph of a 200 nm-period grating with λ/4-shift (arrow) etched in InP*

Resist was stripped by a short etch in buffered HF followed by O_2 RIE
Scale bar = 1 μm

The DLC layer was stripped by a short (5–10 s) etching in 1 : 3 buffered HF : water solution which removes the thin layer of SiO_2 formed on the resist surface by the oxidation of PBTMSS during O_2 RIE. The DLC layer was then removed by O_2 RIE.

Discussion: The resist system and process described in this work constitute a significant improvement over other reported processes in that it combines one of the fastest practical e-beam resists reported to date with the exceptional chemical and mechanical stability of the DLC films. The effective e-beam dose necessary to expose a 200 nm-period grating pattern over larger areas was 3·5 μC/cm^2. The dose necessary to expose an identical pattern in SNR resist[8] and PMMA[6] was 120 and 300–400 μC/cm^2. These values indicate that the pattern-writing time in PBTMSS is, respectively, 35 and 100 times faster than in the two above-mentioned high-resolution e-beam resists.

Thus, we have been able to take full advantage of the high resolution of a modern e-beam lithography system while maintaining the pattern-writing time within acceptable limits (several hours for a full 5 mm × 5 mm 200 nm-period grating area). It is noteworthy that the writing time was not limited by resist sensitivity, which permitted operating the e-beam writing machine close to its maximum operating speed.

The superior performance characteristics of the DFB-DCPBH lasers incorporating gratings fabricated using the process described in this paper are reported elsewhere.[12]

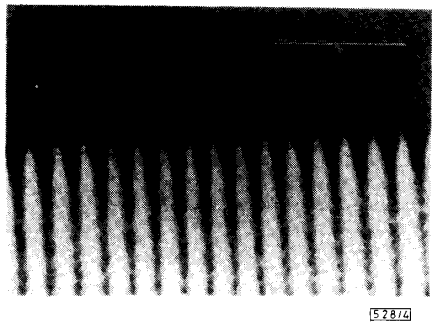

Fig. 4 *SEM micrograph of a 200 nm-period grating etched in InP by Ar^+-beam-assisted etching with ICl vapour*

Resist was stripped as described in Fig. 3
Scale bar = 1 μm

Suffice it to mention that the threshold current of the laser (17 mA) and the minimum linewidth (4·4 MHz at 15 mW) are among the best values reported so far for these devices.

Acknowledgments: We thank J. Osinski for his contribution to wet etching of InP. Close collaboration with C. E. Zah, C. Caneau, S. Menocal and F. Favire is gratefully acknowledged, as are discussions with M. J. Bowden and T. P. Lee.

A. S. GOZDZ
P. S. D. LIN
A. SCHERER
S. F. LEE*

Bell Communications Research
331 Newman Springs Road
Red Bank, NJ 07701, USA

* Present address: Department of Electrical Engineering, Princeton University, Princeton, NJ, USA

2nd December 1987

References

1 NG, W. W., HONG, C.-H., and YARIV, A.: 'Holographic interference lithography for integrated optics', *IEEE Trans.*, 1978, **ED-25**, pp. 1193–1200
2 KOYAMA, F., SUEMATSU, Y., KOJIMA, K., and FURUYA, K.: '1·5 μm phase adjusted active distributed reflector laser for complete dynamic single-mode operation', *Electron. Lett.*, 1984, **20**, pp. 391–393
3 UTAKA, K., AKIBA, S., SAKAI, K., and MATSUSHIMA, M.: 'λ/4-shifted InGaAsP/InP DFB lasers by simultaneous holographic exposure of positive and negative photoresists', *Electron. Lett.*, 1984, **20**, pp. 1008–1010
4 HIRATA, S., TAMAMURA, K., MORI, Y., and KOJIMA, C.: 'AlGaAs/GaAs distributed feedback lasers with first-order grating fabricated by metaloorganic chemical vapor deposition', *Appl. Phys. Lett.*, 1987, **51**, pp. 63–65
5 CRAIGHEAD, H. G., HOWARD, R. E., JACKEL, L. D., and MANKIEWICZ, P. M.: '10 nm linewidth electron beam lithography on GaAs', *Appl. Phys. Lett.*, 1983, **42**, pp. 38–40
6 FICE, M. J., AHMED, H., and CLEMENTS, S.: 'Fabrication of first-order gratings for 1·5 μm DFB lasers by high voltage electron-beam lithography', *Electron. Lett.*, 1987, **23**, pp. 590–592
7 LIN, B. J.: 'Multilayer resist systems', *in* WILLSON, C. G., THOMPSON, L. F., and BOWDEN, M. J. (Eds.): 'Introduction to microlithography', *ACS Symp. Series*, **219**, ACS, Washington, DC, 1983, pp. 304–350
8 KAKUCHI, M., HIKITA, M., and TAMAMURA, T.: 'Amorphous carbon films as resist masks with high reactive ion etching resistance for nanometer lithography', *Appl. Phys. Lett.*, 1986, **48**, pp. 835–837
9 GOZDZ, A. S., CARNAZZA, C., and BOWDEN, M. J.: 'Poly(3-butenyltrimethylsilane sulfone): a sensitive positive electron-beam resist for two-layer systems', *Proc. SPIE*, 1986, **631**, pp. 2–7
10 GOZDZ, A. S., DIJKKAMP, D., SCHUBERT, R., WU, X. D., KLAUSNER, C., and BOWDEN, M. J.: 'Degradation and passivation of poly(alkenylsilane sulfone)s in oxygen plasmas', *in:* 'Polymers for high technology: electronics and photonics', BOWDEN, M. J., and TURNER, S. R. (Eds.), *ACS Symp. Series*, **346**, ACS, Washington, DC, 1987, pp. 334–349
11 TSAI, H.-C., and BOGY, D. B.: 'Characterization of diamondlike carbon films and their application as overcoats on thin-film media for magnetic recording', *J. Vac. Sci. Technol.*, 1987, **A5**, pp. 3287–3312
12 ZAH, C. E., CANEAU, C., MENOCAL, S. G., LIN, P. S. D., GOZDZ, A. S., FAVIRE, F., and LEE, T. P.: 'Narrow-linewidth, 1·3 μm DFB-DCPBH lasers with λ/4-shifted first-order gratings fabricated by electron beam lithography using a new fast resist', *Electron. Lett.*, 1988, **24**, pp. 94–96

EXTREMELY WIDEBAND WAVEGUIDE POLARISER SYSTEM FOR POLARISATION ALIGNMENT

Indexing terms: Polarisation, Satellite links, Telecommunications, Antennas

The letter reports on a system consisting of two quarter-wave polarisers in tandem for polarisation alignment of linearly polarised satellite signals. The signal can be received with the correct polarisation simply by rotating the polariser which is closest to the feed horn. The required isolation in the frequency bands 10·95–12·75 GHz (Rx) and 14·0–14·5 GHz (Tx) is 35 dB on the axis for the total antenna system consisting of reflectors, horn, polariser system and orthomode transducer. This requirement cannot be met when existing polarisers are used and when a ±90° rotation is required. By using a new type of polariser, 38 dB isolation has been measured for the polariser system over the entire frequency band and over the entire range of rotation, with transmission loss below 0·15 dB and return loss below −25 dB (VSWR < 1·12). The total length of the system is approximately 300 mm.

Introduction: A new business communication system, NORSAT B, is under development in Norway. The system uses linear polarisation both for the downlink (10·95–11·20, 11·45–11·70, and 12·50–12·75 GHz) and uplink (14·0–14·5 GHz). Since the system can communicate via different satellites, and each satellite signal may be polarised in one of the two orthogonal directions, the ground station antenna should be able to be aligned to the correct polarisation orientation. The ground station antenna should also be compatible with other satellite systems using linear or circular polarisation, e.g. TELE-X.

The principles for polarisation alignment or polarisation rotation are well known. One method is to use a system of wire grids between the feed horn and the reflectors to rotate the polarisation. The same rotation without moving the rest of the antenna system can also be achieved by using the polariser system discussed in this paper. The first quarter-wave polariser which is between the horn and the second quarter-wave polariser, can be rotated independently of these (see Fig. 1) to perform the alignment. A third method is to perform the alignment electronically behind the orthomode transducer without moving any part of the antenna system. The last and trivial method is of course to rotate the entire feed or antenna system mechanically.

The simplest and least expensive method for the alignment is probably to apply a polariser system. (This system can be used for circular polarised signals as well as simply replacing one of the polarisers by a waveguide section.) However, with existing polarisers the isolation requirement, which is 35 dB on the axis for the entire antenna system consisting of reflectors, horn, polariser system and orthomode transducer, cannot be met when a ±90° polarisation rotation is required. A new waveguide polariser has therefore been used,[1] having considerably larger bandwidth than can be obtained in existing wideband polarisers.[2]

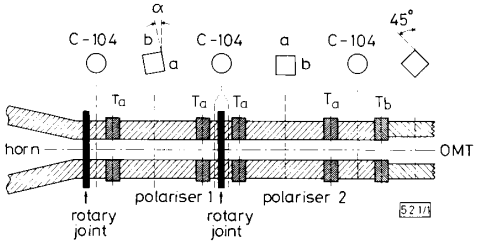

Fig. 1 *Illustration of the polariser system*

Principle of operation: The polariser system consisting of two equal polarisers in tandem is shown in Fig. 1. The linearly polarised signal from the satellite is transformed to have circular polarisation after propagating through polariser 1, and linear polarisation after propagating through polariser 2. Polariser 1 can be rotated independently of the rest of the system, defined by the angular position α. The resulting linearly polarised signal at the OMT-port will then have a relative orientation α compared to the polarisation of the incoming signal in the horn.

If $\Delta\varphi_1$ and $\Delta\varphi_2$ denote the phase difference between the two orthogonal fundamental modes when propagating through polariser 1 and 2, respectively, the isolation I between the modes (crosspolarisation $XP = -I$) can be expressed by

$$I = -10 \log_{10}\left[\frac{(\sin\delta_+ \cos\alpha)^2 + (\sin\delta_- \sin\alpha)^2}{(\cos\delta_+ \cos\alpha)^2 + (\cos\delta_- \sin\alpha)^2}\right] \quad (1a)$$

$$\simeq -10 \log_{10}\left[\delta_+^2 \cos^2\alpha + \delta_-^2 \sin^2\alpha\right]$$

$$\delta_+, \delta_- \text{ small} \quad (1b)$$